Environmental Processes (2022) 9: 8
https://doi.org/10.1007/s40710-021-00553-9

ORIGINAL ARTICLE

Time-Varying Univariate and Bivariate Frequency Analysis of Nonstationary Extreme Sea Level for New York City

Ali Razmi[1] · **Heydar Ali Mardani-Fard**[2] · **Saeed Golian**[1,3] · **Zahra Zahmatkesh**[4]

Received: 14 March 2021 / Accepted: 18 October 2021 / Published online: 26 January 2022

Abstract
Bivariate frequency analysis is an emerging method for the assessment of compound floods, especially in coastal regions. Changing climate, which usually leads to changes in characteristics of extreme hydrometeorological phenomena, makes the application of nonstationary methods more critical. In this research, a methodology is developed to apply frequency analysis on extreme sea level using physically-based hydroclimatic variables as covariates based on univariate Generalized Extreme Value (GEV) as the probability distribution function and copula methods. The results show that for extreme sea level, the location parameter of marginal distribution is directly related to the covariate variable of maximum temperature. For precipitation, the scale parameter is related to the covariate variable of minimum temperature, and the shape parameter is time-dependent. The univariate return periods of hurricanes Sandy and Irene are estimated at 85 and 12 years in nonstationary GEV distribution, respectively, while for stationary GEV distribution they are estimated at 1200 and 25 years, and in the bivariate frequency analysis of water level and precipitation, the normal copula function has more flexibility compared to other competitors. Using time-varying copula, the bivariate return periods of Hurricanes Sandy and Irene are 109 years and 136 years, respectively. The results confirm the importance of incorporating rainfall and extreme sea level in coastal flood frequency analysis. Although the proposed methodology can be applied to other hydro-climatological variables, the findings of this research suggest the necessity of considering nonstationarity in the analysis of extreme hydrologic events.

Keywords Time-Varying Copula · Climate Extreme Event · Dynamic Return Period · Frequency Analysis

1 Introduction

During the past decades, several major flood events have been occurred all over the globe, for example in central Europe in 2002 and 2005, and on the East Coast of the United States in 2011, 2012 and 2017, which resulted in substantial damages (Kron

✉ Heydar Ali Mardani-Fard
h_mardanifard@yu.ac.ir

Extended author information available on the last page of the article

2005; Karamouz et al. 2016, 2017). In the United States, trends for annual flood damages since 1934 suggest that the magnitude and frequency of floods have been increased over the last century (Milly et al. 2002; Svensson et al. 2005; Karamouz et al. 2017). Population and urban growth in floodplains as well as potential social and economic damages from flooding consist incentives to enhance understanding of the major drivers for changes and trends in hydrologic variables. Climate change, for example, has been shown to adversely impact the hydrologic cycle, and therefore, can be related to the increased frequency and magnitude of extreme hydrologic events (Goharian et al. 2016; Zahmatkesh et al. 2015a, b).

The frequency analysis on hydrologic variables is generally performed based on the extreme value analysis of a sample from historical records (Razmi et al. 2017; Mudersbach and Jensen 2010). For hydrologic variables such as temperature and rainfall and also sea level, the extreme value theory (EVT) has been widely used in the literature (e.g., Fréchet 1928; Gumbel 1958; Pickands 1975; Hawkes et al. 2008; Cantet and Arnaud 2014). Among several distributions which have been suggested to fit extreme data (Singh and Strupczewski 2002), according to Abida and Ellouze (2008), the most common probability distributions for flood analysis are Gumbel, Generalized Extreme Value, Log Pearson Type III, and Log-Normal. The principal goal of frequency analysis is to use probability distributions to relate the magnitude of extreme variables to their frequency of occurrence (Gilroy and McCuen 2012), generally based on several assumptions, e.g., data independency, homogeneity and stationarity (Serinaldi and Kilsby 2015). However, there is a debate that climate change could potentially alter the spatial and temporal pattern of hydrologic variables and consequently flooding (Ferrer et al. 2012; Yoon et al. 2015). Changes in the patterns of hydrologic variables affect flood timing, magnitude, and frequency. In designing water system structures for future proper operation and preparedness against flooding, trend analysis of hydrologic variables is necessary. Understanding trends is necessary for identifying the spatial and temporal changes in climatic data. For example, Chebana et al. (2013) performed multivariate hydrologic frequency analysis by emphasizing the importance of application of nonparametric trend tests and recommended jointly applying univariate and multivariate tests to better capture the trend components and select the appropriate models.

Nonstationarity in hydrologic variables and extremes have been investigated in several research studies (Akbari and Reddy 2020; Galiatsatou et al. 2019; Machado et al. 2015; Faulkner et al. 2019; Du et al. 2015; Jiang et al. 2014; Li et al. 2019; Wen et al. 2019; Zhang et al. 2018; Razmi et al. 2017; Dong et al. 2019; Xavier et al. 2019). Ahn and Palmer (2016) for instance, investigated nonstationary frequency analysis of bivariate characteristics, such as occurrence and severity, for annual low flow in the Connecticut River Basin, USA. Yan et al. (2017) developed an approach to derive the nonstationary distribution of runoff and hydrological input including precipitation and potential evaporation. Zhang et al. (2018) developed univariate and bivariate models for time-varying nonstationary frequency of flood peak and volume for Wangkuai Reservoir catchment, in China.

In a review of developments in nonstationary hydrological frequency analysis, several factors, such as changes in river basins by anthropogenic effects, climate change, and low-frequency climate variability were the main reasons for nonstationarity and the assumption of stationarity has been questioned. Bayazit (2015) concluded that relationships between nonstationary model parameters and time should not be only estimated from the data using statistical methods, but need to be defined a priori based on physical mechanisms, which generally includes fitting a probability density function with parameters dependent upon either time and physical drivers of nonstationarity.

Coastal areas are threatened by inland flooding from river overbanking and intense runoff, as well as heavy storms and hurricanes. Compound floods which are caused by multiple drivers can cause devastating damages especially at riverine and coastal regions. To form a compound flood event, multiple drivers or mechanisms such as the combination of rainfall and storm surge as well as pluvial (direct runoff) and fluvial (increased river discharge) are involved (Wahl et al. 2015). Extreme sea levels are caused by combination of physical processes with different time and space scales including tides, sea level rise, weather-driven storm surges and waves, and finally, seasonal and inter-annual variability in ocean water levels. The exceedance probability of extreme sea level and hydrologic variables affecting inland flooding (e.g., rainfall and temperature) is therefore required to be calculated for these areas. The multivariate frequency analysis with copula functions is a good alternative (Tsakiris et al. 2015). For this purpose, application of joint probability distributions such as copulas has been suggested and practiced (Song et al. 2004; Golian et al. 2012; Graler et al. 2013; Roussas 2014; Guo et al. 2016). Copulas have also been used in design of structures at coastal areas. Xu et al. (2014) used copula for joint analysis of extreme precipitation and storm tide, and developed a design standard for preparedness against future flooding. Zellou and Rahali (2019) investigated the combined effect of heavy rainfall with high tidal levels on the occurrence and severity of floods using copulas in a watershed near the Bouregreg River, Morocco. Some recent studies also applied copulas for nonstationary frequency analysis, e.g., Kang et al. (2019) developed a time-varying copula model for bivariate modeling of flood peak and volume. Many studies have been conducted to evaluate historical compound floods around the world, for example Hurricane Irene and Sandy (Saleh et al. 2017), Typhoon Maemi (Lee et al. 2019), Cyclone Sidr (Ikeuchi et al. 2017), and Hurricane Isabel (Blanton et al. 2018). Recently, many efforts have been made to study the impact of climate change on compound flooding (Herdman et al. 2018; Kirkpatrick and Olbert 2020; Pasquier et al. 2018). The time-varying copula modeling is applied to analyze compound extremes and flood event coincidence analysis. In limited studies (e.g., Sarhadi et al. 2016; Kang et al. 2019; Xu et al. 2019; Wen et al. 2019; Feng et al. 2020), time-varying copulas were applied to compound flood frequency analysis.

This paper provides a framework for trend detection, univariate and multivariate frequency analysis, and joint probability distribution of hydrologic variables, i.e., precipitation and extreme sea level using time, maximum and minimum temperature as potential covariates. Historical extreme climate variables and extreme sea level for the coastal area of New York City, southern Manhattan, are used to implement the proposed framework. While Razmi et al. (2017) proposed a uni-variate nonstationary frequency analysis on extreme sea level, this paper promotes the previous work by developing bivariate time variant frequency analysis for compound coastal floods based on nonstationary probability distribution of marginal variables. Also, to consider nonstationarity in the parameters of the bivariate joint distribution of rainfall and extreme sea level, both static and dynamic copula methods are applied. In this study, for the first time, we considered all possible combinations for both parameters of marginal and copulas to be nonstationary/time-varying simultaneously. While in most previous studies, one or more parameters of marginal distribution (usually shape parameter in GEV distribution) have been considered to be constant (Coles 2001; Fowler et al. 2010; Katz 2013; Lopez and Frances 2013; Cheng et al. 2014; Du et al. 2015; Luo and Zhu 2019; Zavier et al. 2019; Le Roux et al. 2020; Lu et al. 2020), we examine cases where the shape parameter can also vary with time and other covariates, i.e., maximum and minimum temperature (Brown et al. 2014; Ouarda et al. 2019; Griffin et al. 2019; Prosdocimi and Kjeldsen 2021). In our study, we developed stationary/nonstationary

models using different copula families, i.e., Archimedean and elliptical copula families, and we applied them to coastal floods. The structure of the paper follows. In the next section, the study area and historical observed data are presented. Then, the methodology is described with the proposed flowchart for the statistical analysis of variables. This section is followed by providing and discussing the results. Finally, a summary and conclusion is given.

2 Study Area and Data

Manhattan, the most densely populated region of the five boroughs of New York City (NYC), with an area of 87.46 km^2 and 1.63 million residents (recorded in 2018), is surrounded by waterways all around and is threatened by flooding from heavy rainfall and storm surges. More than 30 storm events have hit the east coast of the United States, including NYC, since the seventeenth century. The deadliest events that affected Manhattan in the past decade are hurricane Irene and super storm Sandy both with high-speed winds of up to 110 km/h. Hurricane Irene of August 2011 was recorded as one of the most destructive and costliest cyclones. Sandy of October 2012 was a late-season large storm (largest ever recorded in the Atlantic Basin) which flooded some parts of Sothern Manhattan including tunnels and subway systems. According to data from the Battery Park station in the southern part of Manhattan (Fig. 1), the extreme sea level in southern Manhattan due to super storm Sandy was recorded as high as 5.28 m (based on Station Datum). Statistical analysis of extreme sea level at this station indicates a long-term average of 3.28 m. For this study, trend detection and flood frequency analysis were performed on rainfall and extreme sea level data for Manhattan. These data are recorded at the Central Park and the Battery Park stations shown in Table 1.

3 Methodology

Figure 2 shows a flowchart of the proposed methodology for time-varying joint probability density of rainfall with extreme sea level. The methodology includes four main steps namely data collection and processing, trend analysis, frequency analysis, and determination of return period of extreme events. These steps are described in detail in this section.

3.1 Data Collection and Processing

Daily data time series for rainfall (cumulative rainfall over 24 h for each day), the maximum hourly extreme sea level in a day, and temperature (maximum and minimum values over the day), were used for statistical analysis. The data were investigated and then time series of extreme annual data were built for further analysis.

3.2 Trend Analysis

Mann–Kendall (MK) test is the well-known choice to detect the trend in a univariate time series. On the other hand, when weather conditions (e.g., rainfall) potentially influence time series of the variable of interest (i.e., extreme sea level), an appropriate choice

Fig. 1 The location of the Battery Park and Central Park Stations in Manhattan

Table 1 Datasets and characteristics of the stations to acquire data

Station	Longitude	Latitude	Elevation (m)	Record period	Data
Battery Park	74°00′48″	40°42′00″	15.24	1920–2019	Extreme sea level (m)
Central Park	73°57′55″	40°46′56″	39.6	1920–2019	Rainfall (mm), maximum and minimum temperature (°C)

for trend analysis could be the Partial Mann–Kendall (PMK) test (Libiseller and Grimvall 2002). Details of MK and PMK test are given in Section 1 of the Supplementary Material (SM). The PMK test detects trend in a variable (often called response variable) while adjusting for trend in a covariate (Wahlin and Grimvall 2009). In the present study, time series of rainfall was used as the covariate in the analysis and the PMK test statistic was computed conditional on the rainfall. In other words, trend analysis of extreme sea level was investigated while incorporating rainfall as the covariate.

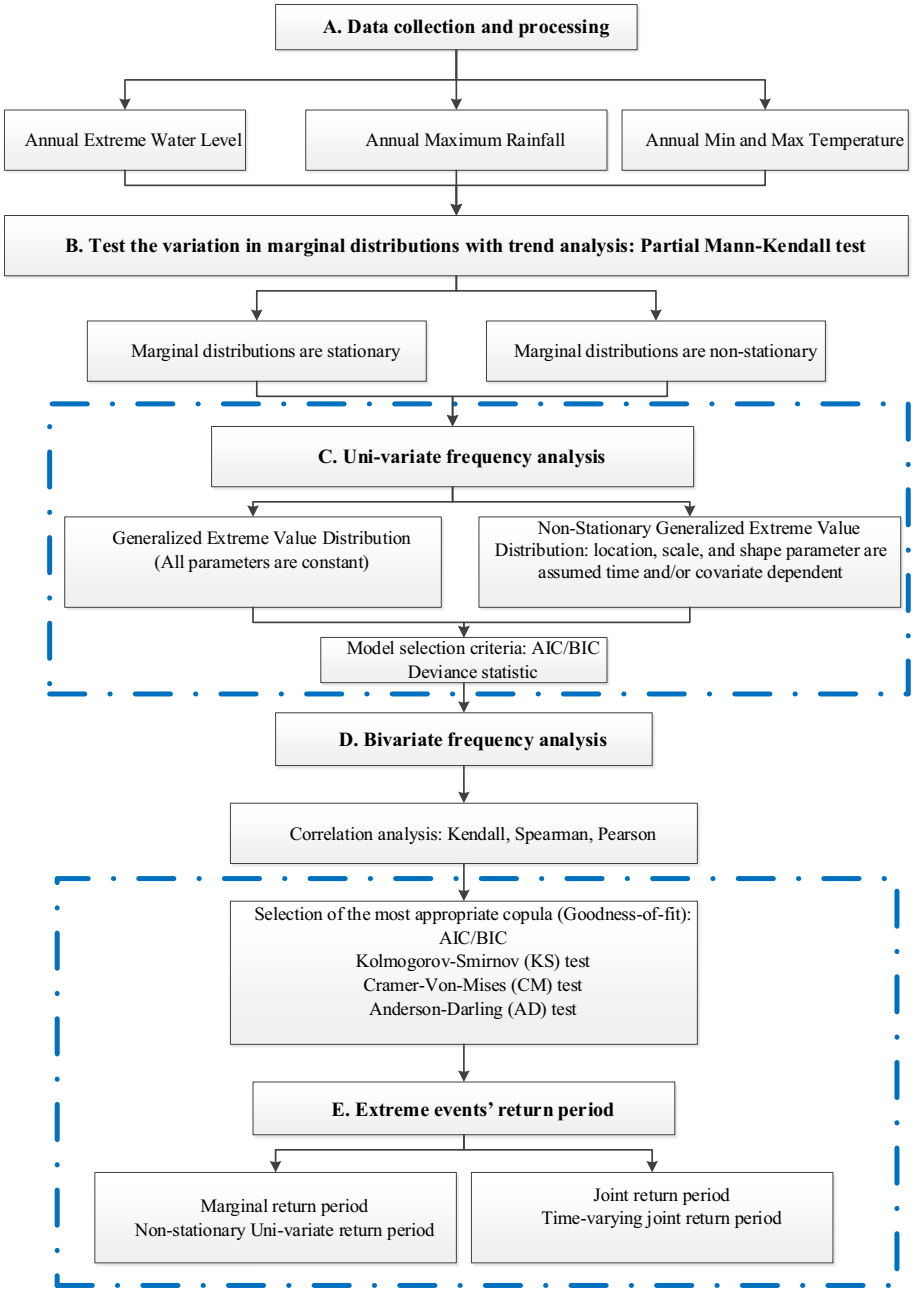

Fig. 2 Flowchart of the proposed methodology to estimate the joint return period of extreme hydrologic variables

3.3 Univariate Frequency Analysis: Static and Dynamic GEV Distribution

Standard design methods are usually based on univariate frequency analysis (Chebana and Ouarda 2011). In this study, the univariate Generalized Extreme Value (GEV) is examined for extreme sea level and precipitation. We use maximum and minimum temperature as covariates. GEV distribution is parameterized with location (μ), scale (σ), and shape (ξ). The density function of the static GEV distribution is expressed as:

$$f_X(x;\mu,\sigma,\xi) = \frac{1}{\sigma}\left[1+\xi\left(\frac{x-\mu}{\sigma}\right)\right]^{-\frac{1}{\xi}-1} exp\left\{-\left[1+\xi\left(\frac{x-\mu}{\sigma}\right)\right]^{-\frac{1}{\xi}}\right\}. \quad (1)$$

The density function of time-varying GEV distribution could be expressed as follows:

$$f_{X_t}(x;\mu_t,\sigma_t,\xi_t) = \frac{1}{\sigma_t}\left[1+\xi_t\left(\frac{x-\mu_t}{\sigma_t}\right)\right]^{-\frac{1}{\xi_t}-1} exp\left\{-\left[1+\xi_t\left(\frac{x-\mu_t}{\sigma_t}\right)\right]^{-\frac{1}{\xi_t}}\right\}, \quad (2)$$

where μ_t, σ_t, and ξ_t are the time-varying location, scale, and shape parameters, respectively (Sarhadi and Soulis 2017). The relation between parameters and time is considered logarithmic with the reference year 1919, i.e., $\ln(year-1919)$ is used as time in the model. The linear relation is also checked but the logarithmic model was fitted better for both variables. Each parameter can be constant, linear in the log of time, linear in covariate, and linear in both log of time and covariate. However, we have not used both covariates in a single model, simultaneously. There are 120 such distinct models for each target variable. The scheme of these 120 models is given in Table 2. Finally, for range preservity of estimations, when fitting the models, a log transform and a logit transform were performed on

Table 2 120 distinct models for GEV distribution for a target variable y with covariates x_1 and x_2

Model	Location (μ_y)	Scale (σ_y)	Shape (ξ_y)	
M_1	μ_0	σ_0	ξ_0	(a)
M_2			$\xi_0+\xi_1\ln t$	(b)
M_3			$\xi_0+\xi_1+\xi_1 x_1$	(c)
M_4			$\xi_0+\xi_1\ln t+\xi_2 x_1$	(d)
M_5			$\xi_0+\xi_1 x_2$	(e)
M_6			$\xi_0+\xi_1\ln t+\xi_2 x_2$	(f)
M_7–M_{12}		$\sigma_0+\sigma_1\ln t$	(a)-(f)	
M_{13}–M_{16}		$\sigma_0+\sigma_1 x_1$	(a)-(d)	
M_{17}–M_{20}		$\sigma_0+\sigma_1\ln t+\sigma_2 x_1$	(a)-(d)	
M_{21}–M_{24}		$\sigma_0+\sigma_1 x_2$	(a),(b),(e),(f)	
M_{25}–M_{28}		$\sigma_0+\sigma_1\ln t+\sigma_2 x_2$	(a),(b),(e),(f)	
M_{29}–M_{56}	$\mu_0+\mu_1\ln t$	same as models M_1–M_{28} (28 models)		
M_{57}–M_{72}	$\mu_0+\mu_1 x_1$	all models M_1–M_{28} except those which σ or ξ depends on x_2 (16 models)		
M_{73}–M_{88}	$\mu_0+\mu_1\ln t+\mu_2 x_1$	same as models M_{57}–M_{72} (16 models)		
M_{89}–M_{104}	$\mu_0+\mu_1 x_2$	all models M_1–M_{28} except those which σ or ξ depends on x_1 (16 models)		
M_{105}–M_{120}	$\mu_0+\mu_1\ln t+\mu_2 x_2$	same as models M_{89}–M_{104} (16 models)		

scale and shape parameters, respectively: we model $\ln\sigma$ and $\text{logit}\left(\frac{2}{3}(\xi+1)\right)$ instead of σ and ξ, itself, where $\text{logit}(x) = \ln(x/(1-x))$.

3.4 Multivariate Frequency Analysis

Application of univariate frequency analysis methods may result in significant underestimation of the risk associated with the considered extreme event. To take into account the mutual information of considered variables, the concept of copula is used. Details on the theory of copulas and its parameter estimation are provided in Supplementary Material. Briefly, copulas are the multivariate distribution functions with standard uniform marginal distributions. Sklar theorem (Sklar 1959) relates the bivariate distribution function to the copula and marginal distribution functions: if X and Y are distributed with cumulative distribution functions (CDFs) F_X and F_Y and bivariate CDF $H(x, y)$, then the copula of X and Y is defined as:

$$C_{X,Y}(u, v) = H\left(F_X^{-1}(u), F_Y^{-1}(v)\right), \tag{3}$$

where F_X^{-1} and F_Y^{-1} stand for the quantile function of X and Y, respectively. In practice, to fit a copula to the data, first, the marginal distribution functions are estimated, e.g., through fitting with nonstationary GEV distribution. Then, $u_i = F_X(x_i)$ and $v_i = F_Y(y_i)$ are computed and, finally, an appropriate copula is fitted to observations (u_i, v_i), $i = 1, 2, \ldots, n$. The density of a copula, $c(u, v)$ is expressed as:

$$c(u, v) = \frac{\partial^2 C(u, v)}{\partial u \partial v}, \tag{4}$$

in which $\partial C/\partial u$ is the partial derivative of C with respect to u. The conditional copula of U given $V = v$ is defined as:

$$C_{U|V=v}(u, v) = \frac{\partial C(u, v)}{\partial v}. \tag{5}$$

It is well-known that the random variable $W = C_{U|V=v}(U, v)$ is uniformly distributed on $(0, 1)$. It can be used in the goodness-of-fit test for dynamic copulas. The Kendall τ for given copula, C, can be computed as (Nelsen 2006):

$$\tau_C = \int_0^1 \int_0^1 C(u, v)c(u, v)dvdu - 1. \tag{6}$$

In this paper, three well-known Archimedean copulas including Clayton, Gumbel, and Frank copula along with normal copula have been used. Details of these copulas are given in the Supplementary Material. All of these copulas are one parameter and there is a one-to-one relationship between their parameters and Kendall τ. For more details, see Nelsen (2006). Note that Clayton, Frank and normal copula with $\theta \cong 0$ and Gumbel copula with $\theta \cong 1$ lead to $\tau \cong 0$ and in these cases the copulas are almost equivalent to the independent copula, $\Pi(u, v) = uv$. Hence, to test the validity of using copulas, the hypotheses $H_0 : \theta = 0$ for Clayton, Frank, and normal, and $H_0 : \theta = 1$ for Gumbel copula are considered when the static copula is used.

Dynamic copula Patton (2006) proposed an $ARMA(1.10)$ model for Kendall τ of time-varying one parameter Archimedean copula. More precisely, he proposed the following model:

$$\tau_t = \Lambda\Big(\alpha + \beta\Lambda^{-1}\big(\tau_{t-1}\big) + \frac{\gamma}{10}\sum_{j=1}^{10}\Big|u_{t-j} - v_{t-j}\Big|\Big) \tag{7}$$

where α, β, and γ are unknown parameters, $\big(u_t, v_t\big) = \big(F_X\big(x_t\big), F_Y\big(y_t\big)\big)$ are the psudo-observations, and $\Lambda(x) = (1 + \exp(-x))^{-1}$ is a transformation function which keeps the value of τ_t in $[0, 1]$. In this paper, the above methodology is used with two modifications: first, instead of Kendall τ, the copula parameter is directly modeled as an $ARMA(1, 10)$ model. i.e.

$$\theta_t = \Lambda\Big(\alpha + \beta\Lambda^{-1}\big(\theta_{t-1}\big) + \frac{\gamma}{10}\sum_{j=1}^{10}\Big|u_{t-j} - v_{t-j}\Big|\Big). \tag{8}$$

The second modification is using new transformation functions, $\Lambda(x)$, which covers a wide range of the parameter space (acceptable values of θ) when x varies in a reasonable range of real numbers. New transformation functions are presented in Table 3. Due to different parameter spaces of different copulas, the transformation functions are also different.

These transformation functions are continuous and differentiable, and as stated above, they vary in a wide range of θ when x varies in a reasonable range of real numbers, e.g., (-10, 10). Although, in theory, the results of Patton's transformation and these new transformation functions are almost the same, in practice, new transformation functions lead to more acceptable and robust results. In summary, the joint distribution function of two hydrologic variables x_t and y_t is modeled as:

$$H\big(x_t, y_t|\theta_t^x, \theta_t^y, \theta_t^c\big) = C\big(F_X\big(x_t|\theta_t^x\big), F_Y\big(y_t|\theta_t^y\big)|\theta_t^c\big) = C\big(u_t, v_t|\theta_t^c\big), \tag{9}$$

where F_X and F_Y are the univariate distribution functions of x and y, respectively; $u_t = F_X\big(x_t\big)$, $v_t = F_Y\big(y_t\big)$, H is the bivariate distribution function of (x_t, y_t); $\theta_t^x = (\mu_t^x, \sigma_t^x, \xi_t^x)$ and $\theta_y^t = (\mu_t^y, \sigma_t^y, \xi_t^y)$ are the vector of time-varying marginal distribution parameters at time t, and θ_t^c is the time-varying parameter of copula function at time t (Sarhadi et al. 2016; Feng et al. 2020). More details are given in Supplementary Material.

3.5 Model Selection (Goodness-of-fit Criterion)

AIC and BIC The well-known goodness of fit criteria when the density function is available, are Akaike Information Criteria (AIC) and Bayesian Information Criteria (BIC). Since

Table 3 Transformation functions for range preservation of copula parameter

Family	$\theta = \Lambda(x)$	$x = \Lambda^{-1}(\theta)$
Gaussian	$\tanh x/2$	$\ln((1+\theta)/(1-\theta))$
Clayton	$\exp x\, I_{\{x<0\}} + [\ln(x+1)+1]I_{\{x\geq 0\}}$	$\ln\theta\, I_{\{0<\theta<1\}} + \big[\exp(\theta-1)-1\big]I_{\{\theta\geq 1\}}$
Frank	x	θ
Gumbel	$\big[\exp x+1\big]I_{\{x<0\}} + [\ln(x+1)+2]I_{\{x\geq 0\}}$	$\ln(\theta-1)I_{\{1<\theta<2\}} + \big[\exp(\theta-2)-1\big]I_{\{\theta\geq 2\}}$

the number of parameters are not equal in all models, the AIC may overestimate the appropriateness of the model, hence, using BIC is more appropriate. The models with lower AIC/BIC are better fitted since they have greater Likelihood value. AIC/BIC can be used for univariate models and copulas. Also, they can be used for both static and time-varying models. More details are given in the Supplementary Material.

Deviance statistic Deviance is a goodness-of-fit statistic for a statistical model which is usually used for statistical hypothesis testing. When two models are nested and the method of estimation is Maximum Likelihood (ML), then using deviance statistic is more efficient. Deviance statistic for comparing models M_0 and M_1 with parameters θ_0 and θ_1, respectively, are defined as follows:

$$D(M_0, M_1) = 2\left(\updownarrow\left(\widehat{\theta}_1\right) - \updownarrow\left(\widehat{\theta}_0\right)\right),$$

where $\widehat{\theta}_0$ and $\widehat{\theta}_1$ are the ML estimators of θ_0 and θ_1, respectively, and $\updownarrow$ is the log-likelihood function. Note that the two models need not to have the same log-likelihood function. The approximate distribution of D is χ^2 with degrees of freedom equal to the difference of number of parameters of θ_1 and θ_0. H_0 means that two models have the same goodness-of-fit, and H_1 means that M_1 is better fitted to the data than M_0. Finally, H_0 is rejected if D is significantly large:

$$\mathrm{H}_0 \text{ is rejected if } \mathrm{D}\left(\mathrm{M}_0, \mathrm{M}_1\right) > \chi^2_{\nu}(\alpha)$$

where ν shows the degrees of freedom explained above, α is the significance level, and $\chi^2_{\nu}(\alpha)$ is the α-th upper quantile of a chi-square distribution with ν degrees of freedom.

Goodness-of-fit test For univariate cases, the most common non-parametric goodness-of-fit tests are Kolmogorov–Smirnov, Anderson–Darling, and Cramer-Von-Mises. To test $H_0 : C = C_0$ when data come from a static copula, a modified test can be used that computes $z_i = C_0\left(u_i|v_i\right)$. Then, under H_0, z_i's would be a sample of the standard uniform distribution, and this can be tested using the above mentioned three methods. When the copula is time-varying, z_i's is not from a single population (Hafner and Manner 2008). Manner and Candelon (2010) proposed a bootstrap-based method to compute the p-value for testing whether $H_0 : C = C^0_t$. More details are given in Supplementary Material.

3.6 Return Periods and Return Levels

For univariate frequency analysis, the relation between return level, $\mathcal{L}$, and its related return period, $\mathcal{P}$, is:

$$\mathcal{L} = F^{-1}(1 - 1/\mathcal{P}), \textit{and } \mathcal{P} = (Pr[X \geq \mathcal{L}])^{-1} = (1 - F(\mathcal{L}))^{-1}.$$

If the fitted distribution is time varying, then the above relations hold for each time epoch, t, separately. Hence, for given return period (level) there is a time-series of return levels (periods) each associated with separate time epoch. In bivariate frequency analysis, the return level is bivariate (i.e., $\mathcal{L} = \left(\mathcal{L}_1, \mathcal{L}_2\right)$) while the return period is still univariate. There are three well-known types of definition for return level: "AND",

"OR", and "Kendall". In this paper, the "AND" return period is used. "AND" return period (level) for given return level (period) is defined as:

$$\mathcal{L}(\mathcal{P}) = \{(x, y) : H(x, y) = 1 - 1/\mathcal{P}\} \text{ and } \mathcal{P}(\mathcal{L}) = \left(Pr\left[X \geq \mathcal{L}_1, Y \geq \mathcal{L}_2\right]\right)^{-1},$$

and in terms of copula:

$$\mathcal{L}(\mathcal{P}) = \left\{(x, y) : C\left(F_X(x), F_Y(y)\right) = 1 - 1/\mathcal{P}\right\} \text{ and } \mathcal{P}(\mathcal{L}) = (1 - u - v + C(u, v))^{-1}.$$

where F_X and F_Y are the univariate CDFs of X and Y, respectively, H and C are their joint CDF and copula, respectively, $u = F_X\left(\mathcal{L}_1\right)$ and $v = G_Y\left(\mathcal{L}_2\right)$. Note that return level of a given return period is a curve in $\mathbb{R}^2$ and it is related to the contours of bivariate distribution function or copula. Clearly, when using time-varying copula, for each time epoch, t, the above relations are valid for each time epoch, separately. More details are given in the Supplementary Material.

4 Results and Discussion

4.1 Trend Analysis

Results for trend analysis of water level and precipitation using MK test are presented in the two first rows of Table 4. Trend analysis of water level as dependent variable was performed using partial MK test considering precipitation in time period 1920–2019. The results for multivariate trend analysis are provided in the last row of Table 4. Based on the p-values in Table 4., the hypothesis of existence of trend is accepted for both variables. Therefore, application of the MK test confirms the existence of trend in the hydrologic data. Also, based on the results of PMK test, it is concluded that there is a trend in water level data based on precipitation.

4.2 Stationary and Time-varying Univariate Frequency Analysis

Model selection Figure 3 shows AIC and BIC for all 120 possible models for each target variable. The most appropriate models were selected based on the BIC criterion (lowest value as indicated in Fig. 3). According to Fig. 3, for target variable water level, best fitted model is M_{106} which is:

$$\mu_{WL} = \mu_0 + \mu_1 \ln t + \mu_2 TMAX; \quad \sigma_{WL} = \sigma_0; \quad \xi_{WL} = \xi_0 + \xi_1 \ln t. \tag{10}$$

This shows that the location parameter is a linear combination of log of time and maximum temperature (TMAX), the scale parameter is constant and the shape parameter is a linear function of log of time. Also, it is clear from the chart that models with time-dependent location parameter have lower AIC/BIC. No general rules were detected for the scale or shape parameters. Note that TMAX is a better covariate for water level than minimum temperature (TMIN). Regarding precipitation, the best model is M_{42}, which is:

$$\mu_{PR} = \mu_0 + \mu_1 \ln t; \quad \sigma_{PR} = \sigma_0 + \sigma_1 TMIN; \quad \xi_{PR} = \xi_0 + \xi_1 \ln t. \tag{11}$$

TMIN is shown to be a better covariate for precipitation. Table 5 contains parameter estimates of the best fitted models as well as the results of the static models. The last column of this table contains deviance statistic for comparing best fitted model to the static model. Time t in this table is $t = year - 1919$ which varies from 1 to 100 for years 1920–2019. The standard errors (numbers in parentheses) were estimated using Monte Carlo method and the significance levels (p-values) were computed through standard t-test. All estimated parameters are statistically significant at level 0.05 and the result of deviance analysis shows that time-varying models fit better than the static model. The plots of time-varying parameters for two target variables are shown in Fig. 4.

Return periods and return levels Return levels of various return periods for static and time-varying univariate distributions in year 2019 are reported in Table 6. Figure 5 shows the return levels associated with return periods 25, 50, 100, and 200 years as well as static model return levels. Also, time-varying return levels are computed and plotted with average covariate value; i.e., by substituting covariates with their 100-year averages in (10) and (11). This smooths the return levels and can be used as the "average time-varying return levels" which does not depend on yearly covariate values. According to these charts, return levels are almost increasing during years 1920–2019.

4.3 Bivariate Frequency Analysis

The dependence structure between extreme sea level and precipitation was investigated using copulas. For this purpose, first, correlation analysis and mutual information was performed using three different methods. Table 7. shows the results of the correlation tests (significance levels are presented in parentheses) and mutual information. Kendall and Spearman correlation coefficients confirm that precipitation has a significant correlation with extreme sea level, but Pearson correlation coefficient is not significant. The mutual information of extreme sea level and precipitation is about 0.31. Note that these results are meaningful only when the static copula models are used.

Parameter estimation and copula selection The marginal distribution functions of variables were estimated using the selected GEV distributions and utilized as inputs for copula estimation. Table 8. shows the estimated parameters for both static and dynamic copulas of extreme sea level and precipitation. In the time-varying analysis, since the objective likelihood functions are not concave, several initial values were used in numerical optimization. The standard errors (numbers in parentheses) were estimated using the Monte-Carlo method. Statistical significance of parameters was examined with the t-test based on asymptotic standard errors. In almost all cases, the static copulas do not fit the data since the estimated parameters are not statistically significant at level 0.05. According to Table 8., parameters of all static copulas are significant at level 0.01. Time-varying Clayton

Table 4 Mann–Kendall test results for univariate trend analysis and partial Mann–Kendall test for conditional trend analysis

Test	Variable	Kendall tau	Z statistic	P-value
MK(Univariate)	WL (m)	0.305	4.37	< 0.001
	PREC (mm)	0.190	2.74	0.006
PMK (Bivariate)	WL and PREC	—	3.71	< 0.001

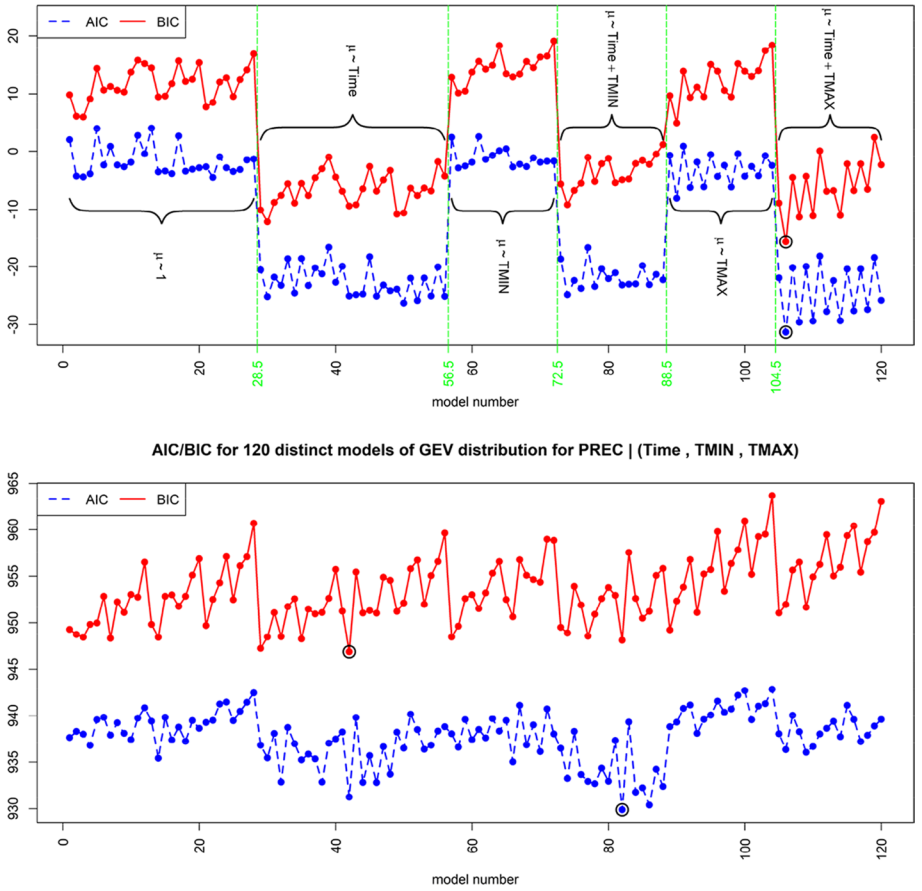

Fig. 3 The AIC and BIC of the 120 distinct GEV models for extreme sea level (top) and precipitation (bottom) (see Table 2). Circle corresponds to the best-fitted model

and Frank copula has only one significant parameter and the parameters of time-varying Gumbel copula are not significant. It can be deduced that these three time-varying copulas do not fit the data well. On the other hand, all three parameters of time-varying normal copula are significant at level 0.01. However, since the standard errors are not exact, these results are not fully reliable and goodness-of-fit criteria should be examined further. The results of goodness-of-fit tests are presented in Table 9. According to Table 9., time-varying normal copula has the minimum BIC value (AIC results are also minimum where the BIC has its lowest values). Also, based on the non-parametric goodness-of-fit tests, the normal copula has larger p-values, and hence, the null-hypothesis is accepted with more certainty. The other three copulas have at least one test with p-value lower than 0.1. Figure 6 shows the estimated static and time-varying parameters of the four copulas, and Kendall correlation coefficients (τ_t) based on static and time-varying copulas are shown in Fig. 7. The non-parametric dynamic estimation of τ_t based on 10 nearest data is estimated and plotted as gray solid line. As expected, the estimated τ_t by time-varying normal copula is very close to the non-parametric one in all cases and the other three copulas have Kendall τ_t near their static Kendallτ.

Table 5 Estimated parameters of the selected models and the static model (numbers in parentheses show the standard errors). Significant parameters at levels 0.05 and 0.01 are marked as * and **, respectively

Target	Selected model	Parameter estimation with the standard error (SE) in parentheses				Deviance
WL	Static model (no covariate)	$\mu_0 = 3.15(0.021)$	$\sigma_0 = -1.646^{**}(0.082)$	$\xi_0 = 0.999^{**}(0.209)$		—
	μ	$\mu_0 + \mu_1 \ln t + \mu_2 TMAX$	$\mu_0 = 3.682^{**}(0.232)$	$\mu_1 = 0.081^{**}(0.008)$	$\mu_2 = -0.022^{**}(0.0039)$	39.35**
	σ	$\exp \sigma_0$	$\sigma_0 = -1.817^{**}(0.092)$			
	ξ	$1.5\,\mathrm{logit}(\xi_0 + \xi_1 \ln t) - 1$	$\xi_0 = -4.027^{*}(1.141)$	$\xi_1 = 1.455^{*}(0.373)$		
PREC	Static model (no covariate)	$\mu_0 = 65.4^{**}(2.38)$	$\sigma_0 = 3.05^{**}(0.084)$	$\xi_0 = 0.875^{*}(0.244)$	—	
	μ	$\mu_0 + \mu_1 \ln t$	$\mu_0 = 42.3^{**}(8.64)$	$\mu_1 = 6.414^{*}(2.33)$		12.381**
	σ	$\exp\left(\sigma_0 + \sigma_1 TMIN\right)$	$\sigma_0 = 2.261(0.318)$	$\sigma_1 = -0.057^{**}(0.022)$		
	ξ	$1.5\,\mathrm{logit}(\xi_0 + \xi_1 \ln t) - 1$	$\xi_0 = -2.863^{**}(0.898)$	$\xi_1 = 0.882^{*}(0.233)$		

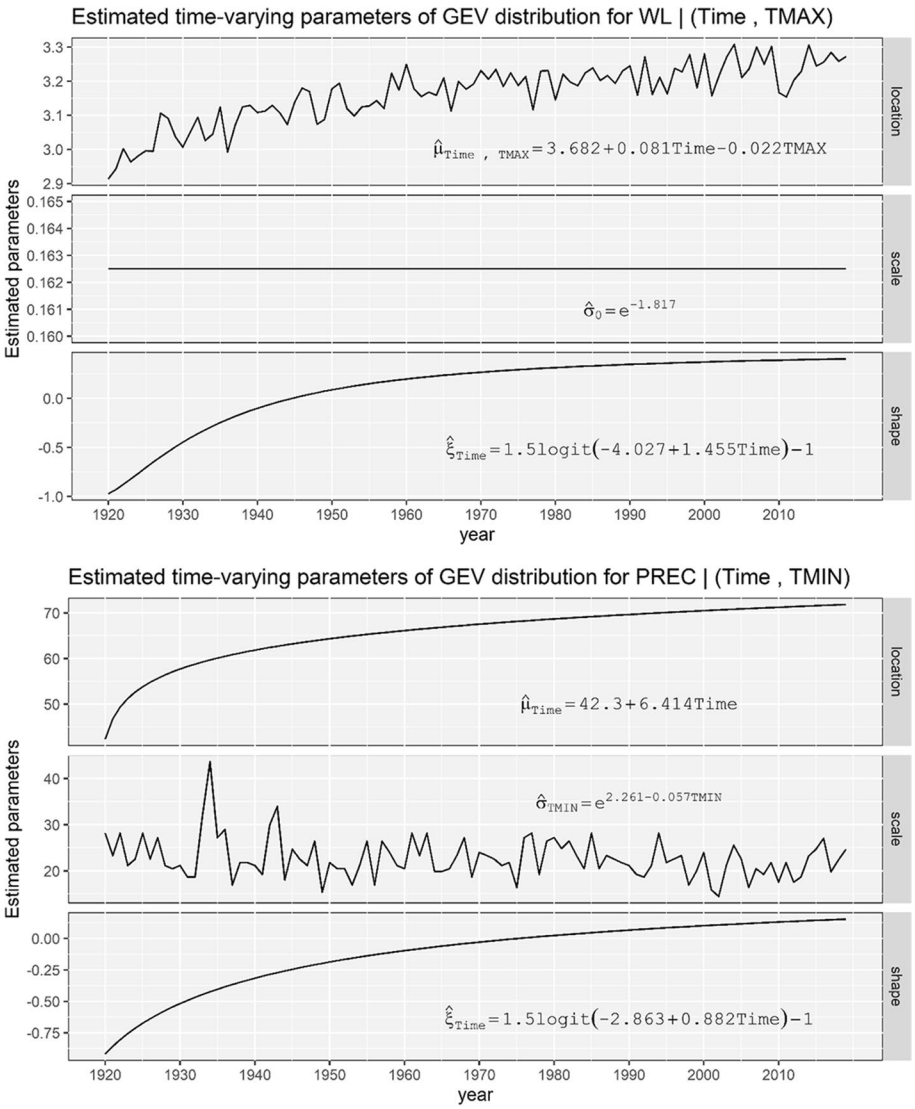

Fig. 4 Plot of estimated time-varying parameters of GEV distribution for extreme sea level (top) and precipitation (bottom). Covariate "Time" represents ln (*year* − 1919)

4.4 Joint Return Levels

Return levels were estimated for return periods of 25, 50, 100, and 200 years. For time-varying models, the copulas of the years 1930, 1960, 1990, and 2019 were used. The normal time-varying copula was selected to estimate the joint return period of extreme sea level and precipitation which is shown in Fig. 8. The univariate return period of Hurricane Sandy is about 85 years based on its extreme sea level and using parameters of year 2019.

Table 6 Return levels of extreme sea level and precipitation at given return periods based on (a) static GEV distribution and (b) time-varying GEV distribution with parameters of year 2019

Return period (year)	WL (m)		PREC (mm)	
	Static	TV	Static	TV
2	3.22	3.34	73.2	81.2
5	3.46	3.61	98.4	113.5
10	3.63	3.88	116.0	138.2
25	3.87	4.33	139.4	173.7
50	4.07	4.81	157.7	203.6
100	4.27	5.45	176.5	236.6
200	4.48	6.28	196.1	273.3
500	4.79	7.81	223.2	327.9
700	4.91	8.52	233.5	350.0
1000	5.04	9.40	244.6	374.7

Univariate return periods of Hurricane Irene are about 12 and 10 years based on its extreme sea level and precipitation levels, respectively, when parameters of year 2019 are used. In fact, Sandy is a "univariate" extreme event in extreme sea level but Irene is essentially a "bivariate" or compound extreme event of (extreme sea level and precipitation), and hence, for Irene, application of the univariate return levels does not seem reasonable. Univariate extreme sea level values higher than that observed for Irene (occurred in 1953, 1960, and 1992) and univariate precipitation values higher than that observed for Irene (occurred in 1966, 1972, 1977 and 2007) and do not show patterns similar to Irene. According to Fig. 8, return period for hurricane Sandy is more than 1000 year based on the parameters of year 1930, while it decreases to 109 years based on parameters of year 2019. In previous studies, the return period for hurricane Sandy was also reported to vary from less than 100 years (Garner et al. 2017) to around 1000 years (e.g., Lin et al. 2012; Karamouz and Farzaneh 2020), and to more than 10,000 years (Shrestha et al. 2014). This shows how different factors, e.g., selection of marginal distribution function, uni/multi-variate methods of frequency analysis, static/time-varying parameters of marginal distributions/copula can affect the results of frequency analysis significantly. This also reveals the importance of considering a flexible method for frequency analysis which can consider different possible combinations of cases in terms of static/time-varying parameters for both marginal distributions and also the copula function itself. Table 10. shows return periods for some extreme events based on the copula of different years, 1930, 1960, 1990, and 2019, as well as with the static copula. It can be easily seen that during time, the predicted return period for such extreme events is in an increasing order. Among these cases, the event of year 2012 is a univariate extreme event of extreme sea level, the events of years 1960 and 2011 are two bivariate extreme events and the events of years 1966, 1972, 1977, and 2007 are univariate extreme events of precipitation. Another important result based on Fig. 8d is that extreme events such as Sandy and Irene could be expected to occur more frequently as a result of factors such as climate variability. It has been recommended by some researchers that risk assessment methods should consider natural hazards, e.g., flood at coastal regions as compound events to take different drivers and/or hazards into account (e.g., Zscheischler et al. 2018) and/or nonstationarity in data should be reflected in frequency analysis methods (e.g., Pirani and Najafi 2020).

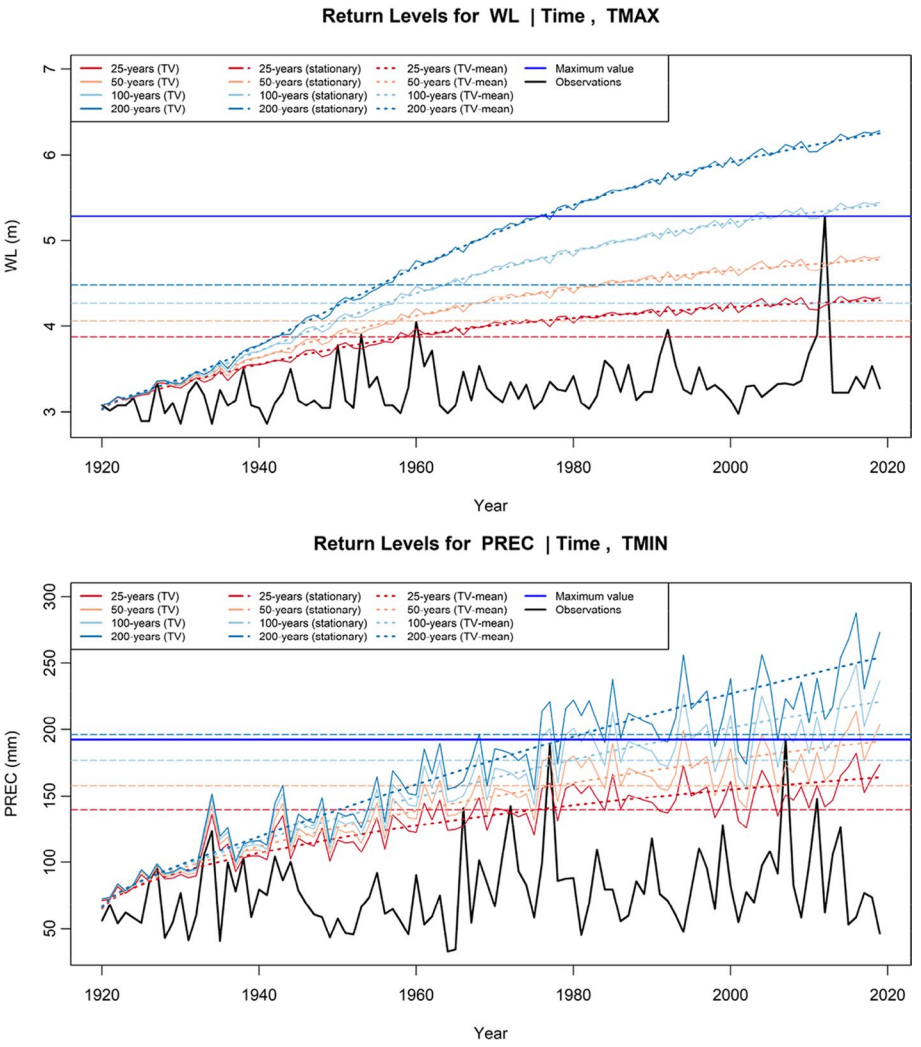

Fig. 5 Univariate return levels of extreme sea level (top) and precipitation (bottom) associated with return periods of 25, 50, 100, and 200 years. Solid black line: data, solid colored: time-varying return level, dashed: static return period, dotted: average time-varying return period, solid horizontal blue line: maximum value of the data

Table 7 Correlation coefficients of extreme sea level and precipitation (* and **: significant at levels 0.05 and 0.01, respectively)

Method	Kendall	Spearman	Pearson	Mutual information
Value	0.186^{**}	0.278^{**}	0.130	0.31

Table 8 Estimated parameters for static and dynamic copulas of extreme sea level and other climate variables. Estimated standard errors are in parentheses. (* and **: significant at levels 0.05 and 0.01, respectively)

Copula	Static copula		Time-varying copula					
	θ		α		β		γ	
Clayton	0.342**	(0.141)	0.851	(2.118)	0.837**	(0.245)	-1.126	(1.753)
Frank	1.229**	(0.4163)	-0.471	(1.892)	0.958**	(0.077)	0.276	(0.699)
Gumbel	1.138**	(0.0453)	-1.045	(1.001)	-0.141	(0.904)	-2.968	(3.943)
Normal	0.25**	(0.0884)	0.040**	(0.019)	-2.837**	(1.296)	1.645**	(0.514)

Table 9 Goodness-of-fit criteria of time-varying copulas: AIC, BIC, and bootstrap-based p-values of modified non-parametric tests for V time-varying copula model

Copula	Criteria				
	AIC	BIC	KS-test	AD-test	CM-test
Clayton	-2.53	5.29	0.034	0.071	0.126
Frank	1.60	9.41	0.035	0.070	0.043
Gumbel	-0.76	7.06	0.130	0.082	0.160
Normal	**-8.34**	**-0.53**	0.258	0.252	0.410

Fig. 6 Estimated time-varying parameters of four copulas. Top to bottom: Clayton, Frank, Gumbel, and normal copula

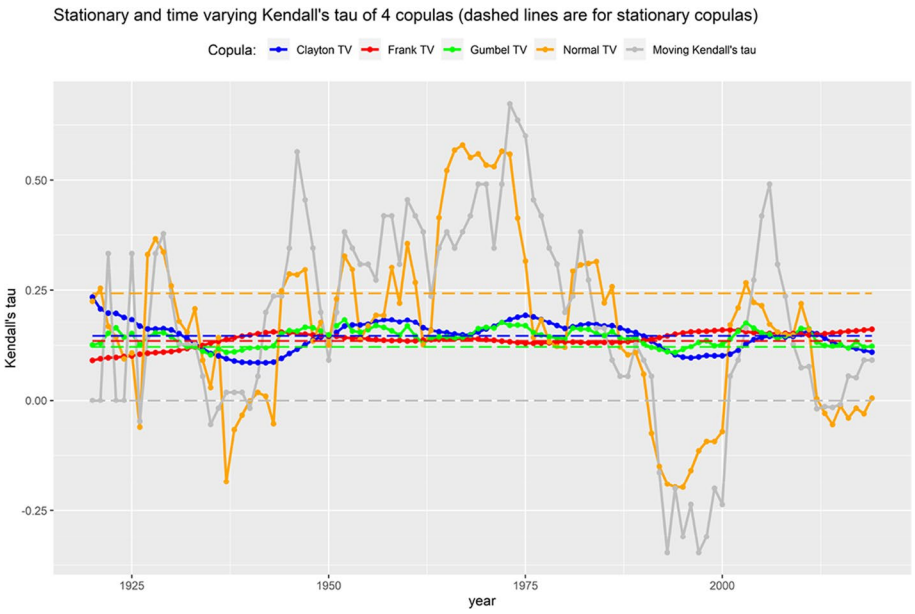

Fig. 7 Estimated time-varying Kendall τ_t for time-varying and static copulas. Blue: Clayton, red: Frank, green: Gumbel, orange: normal. Solid: time-varying, dashed: static. Dynamic non-parametric estimation of Kendalls τ with bandwidth = 10 years is plotted with gray solid line

4.5 Discussion

Compound flooding can arise from three main sources: 1) extreme sea levels (comprised of storm surge, high astronomical tides, and/or waves (coastal flood) and heavy precipitation); 2) river discharge (fluvial flood) and extreme sea levels; and 3) direct surface run-off from rainfall (pluvial flood) and extreme sea levels (Lai et al. 2021; Hendry et al. 2019). Compound flooding is usually induced by the concurrence of extreme sea levels and heavy precipitation, with the former involving oceanic processes and the latter involving hydrological processes (Wahl et al. 2015; Zhang et al. 2020). One of the objectives of this paper was to study combined extreme events that lead to compound floods and the need to review the risk management studies of water infrastructure in the region. As the precipitation of Hurricane Sandy was not heavy enough, it cannot be categorized as a compound flood and the nonstationary univariate frequency analysis can be a good choice for such events. For Hurricane Sandy (exceptional value) the return period under stationary univariate frequency analysis is more than 1000 years while under nonstationary univariate frequency analysis, the return period would reduce to less than 85 years. Using nonstationary bivariate frequency analysis for Hurricane Sandy and using normal copula as the most optimal copula function with parameters for the year 2019, a return period of 109 years was calculated. It should be noted that the amount of rainfall on the day of Hurricane Sandy was less than the average rainfall (78 mm). In a similar study, Lin et al. (2016) found that due to the effect of sea-level rise, the return period of flood caused by Hurricane Sandy decreased by approximately 3 times from year 1800 to 2000, and it is estimated to further decrease by approximately 5 times from 2000 to 2100 under a moderate-emissions pathway. This means that

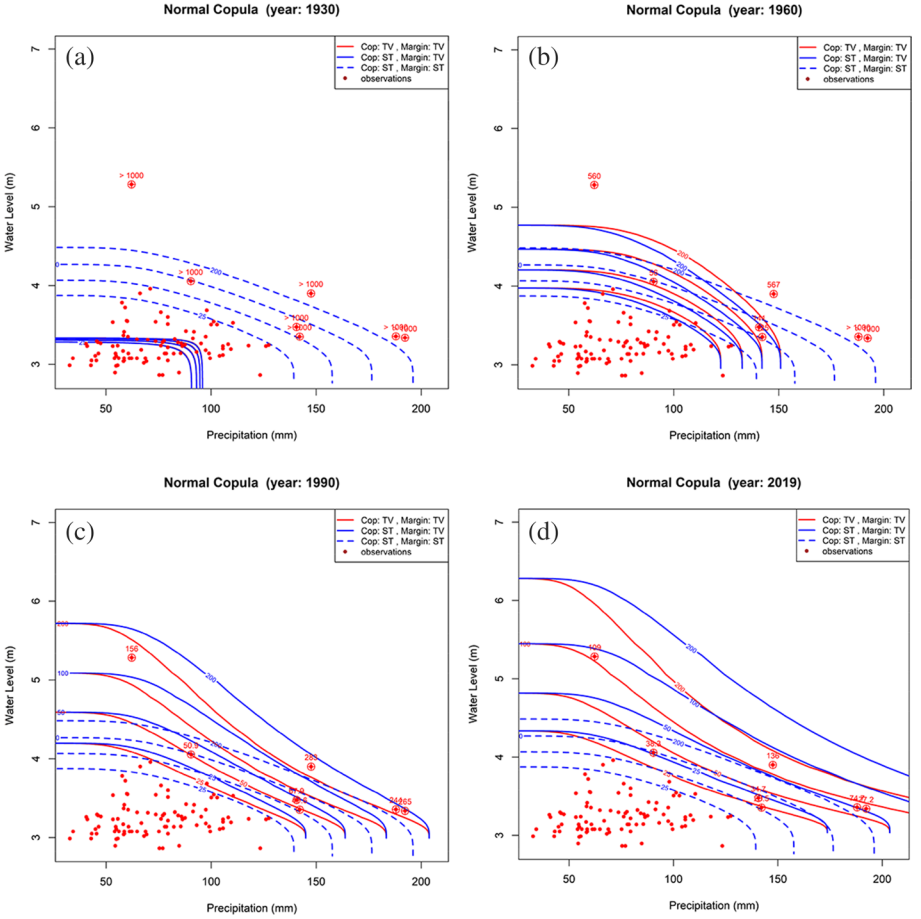

Fig. 8 Joint return levels of extreme sea level and precipitation estimated based on static and time-varying normal copula. Red solid: time-varying copula with time-varying marginal, blue solid: time-varying copula with static marginal, dashed blue line: static copula. Some extreme events (including Irene and Sandy hurricanes) are marked with plus sign and their time-varying return periods are written next to their point. For more details, see Table 10. Base year of time-varying copula: (a) 1930, (b) 1960, (c) 1990, and (d) 2019

Table 10 Return periods of some extreme events based on static and time-varying copula of years 1930, 1960, 1990, and 2019

Year	Precipitation	Water level	Static copula	Copula 1930	Copula 1960	Copula 1990	Copula 2019
1960	90.4	4.05	97	> 1000	56	51	38
1966	140.7	3.48	72	> 1000	141	68	35
1972	142.2	3.35	53	> 1000	125	48	24
1977	188.0	3.36	260	> 1000	> 1000	244	75
2007	192.3	3.34	288	> 1000	> 1000	265	77
2011	147.6	3.90	329	> 1000	567	283	136
2012	62.2	5.28	> 1000	> 1000	560	156	109

the return period of a storm with the same magnitude as Hurricane Sandy can be decreased from 300 to 20 years in 2100. Hurricane Irene, the first major Atlantic hurricane in 2011, made its landfall along the US East Coast at Outer Bank, North Carolina (NC), on Aug 27, 2011. The different flood origins (ocean and inland) made this event an ideal test for compound-flood modeling (Ye et al. 2019). Regarding Hurricane Irene (maximum water level rise 3.89 m), the increase in water level was higher than the average maximum water level rise, i.e., 3.28 m, but its value is far less than Hurricane Sandy. So, Hurricane Irene is not classified as an exceptional storm. However, its occurrence with a heavy rainfall of 147 mm was much higher than the average rainfall of 78 mm, which leads this hurricane to be classified as a compound flood. For Hurricane Irene, the stationary univariate frequency analysis shows a return period of 25 years exactly equal to the return period of water level, but the nonstationary univariate frequency analysis shows a return period of 12 years. The point to be noted here is that the composite flood resulting from Hurricane Irene cannot be traditionally estimated by the univariate frequency analysis method because it is classified as a coincidence (compound) event (Fig. 8). Finally, using nonstationary bivariate frequency analysis for hurricane Irene using normal copula with time-dependent theta parameter equal to its value in year 2019 resulted in a return period of 136 years with category of joint events with extreme sea level and rainfall (compound flood). Based on Fig. 5 (Return levels for WL | Time, TMAX), we can conclude that as we approach the year 2019, water level increases for an identical return period. One reason for this can be related to the effect of sea-level rise on storm tide in the New York area. In Fig. 5, precipitation as main variable has a significant relationship with the minimum temperature in nonstationary conditions, which corresponds to the results of Singh et al. (2021).

The findings presented here are consistent with previous studies conducted in the USA (Wahl et al. 2015) and other regions, such as China (Fang et al. 2020), Europe (Ganguli and Merz 2019), and Canada (Wang 2020), which showed that significant dependence exists between various flood hazard drivers and necessitates the importance of considering all dependent flood drivers in design of drainage systems and other flood mitigation infrastructure. This is of particular importance for New York; our results are in compliance with other studies (Moftakhari et al. 2017; Bevacqua et al. 2019) and indicate that the frequency of compound events is increasing in the coastal regions of New York under climate change, in particular sea-level rise. In this study, we considered two drivers of flooding, i.e., precipitation and extreme sea level with minimum and maximum temperature as covariates. The role of other flooding drivers needs to be further explored, as well as compound effects under nonstationary conditions, including multivariate frequency analysis, assessing the relationship to climate indices, and the implications for flood risk management. The latter is particularly important, given the low capacity of drainage systems in many New York urban areas.

5 Conclusions

Frequency analysis for several hydroclimatic variables including extreme sea level and precipitation as the main variables and maximum and minimum temperature as covariate variables was conducted based on static and time-varying parameter distributions. The coastal region of Manhattan in New York City was selected as the case study. Required data for the analysis were obtained from the Central Park and Battery Park stations.

For univariate and multivariate trend analysis, the Mann–Kendall and Partial Mann–Kendall tests were used, respectively. The joint probability occurrence of marginal extreme sea level and rainfall with minimum and maximum temperature covariate variables was then assessed using several copula functions. Considering the parameters of marginal distribution and copulas to be constant or varying in time, different model combinations were tested in terms of variables and parameter type (constant vs time-varying) and joint probability occurrence of marginal extreme sea level and rainfall were calculated using time, minimum and maximum temperature as potential covariates for different return periods. Results of trend analysis indicated an increase in long term average of precipitation and extreme sea level. This could be attributed to global warming and the impacts of climate change.

The results also showed that the Generalized Extreme Value (GEV) is the most appropriate distribution to fit to the hydrologic variables of the study region. In general, incorporating climate variables in the joint frequency analysis of extreme sea level resulted in decrease in extreme sea level compared to values from the univariate analysis for the same return periods. Considering bivariate frequency analysis when designing hydraulic structures reduces the risk of compound flooding. The results of joint probability distribution analysis showed mutual influence of rainfall variable and extreme sea level. This highlights the necessity of considering climate variables such as rainfall and temperature in coastal flood frequency studies when analyzing extreme sea level data. As time-series used in this analysis includes 100 years of data, it is robust enough to compare and validate the results of this study with empirical frequency analysis.

For assessing the goodness-of-fit of the developed models, log-likelihood statistics such as AIC and BIC were used. Also, in addition to Anderson–Darling (AD), Kolmogorov–Smirnov (KS), and Cramer-Von Mises (CM) tests on transformed data, by Rosenblatt probability integral transform, a parametric bootstrap method was proposed for approximating p-values to take into account the uncertainty of the dependence process. In hydrological risk analysis, there are different design models based on the return periods, so estimating the bivariate return period before building hydraulic or offshore structures could reduce the cost of flood damage, constructing coastal flood defense structures based on bivariate frequency analysis would bring more advantages in favor of possible alternatives.

Based on the results of this study, it is suggested that multivariate frequency analysis models need to be flexible to consider joint variables of all possible types in terms of nonstationarity, e.g., for bivariate analysis: stationary-stationary, nonstationary-stationary, and nonstationary-nonstationary data pairs should be examined. For nonstationary variables, using static copulas could lead to false results. Furthermore, taking into account a range of copula families and selecting the right copula family with a flexible copula parameter (time resilient) very important.

Supplementary Information The online version contains supplementary material available at https://doi.org/10.1007/s40710-021-00553-9.

Authors Contributions Ali Razmi, Heydar Ali Mardani-Fard, and Saeed Golian designed the framework and analyzed the data. Heydar Ali Mardani-Fard and Ali Razmi performed the analysis and modeling. Zahra Zahmatkesh wrote the manuscript with support from Heydar Ali Mardani-Fard and Saeed Golian. Zahra Zahmatkesh and Saeed Golian supervised the research. All authors discussed the results and contributed to the final manuscript.

Funding The authors did not receive support from any organization for the submitted work.

Data Availability All data used to conduct this research are free and available to the public.

Code Availability Some codes generated during this study are available by the corresponding author.

Declarations

Conflicts of interest/Competing interests Not Applicable.

References

Abida H, Ellouze M (2008) Probability distribution of flood flows in Tunisia. Hydrol Earth Syst Sci 12(3):703–714. https://doi.org/10.5194/hess-12-703-2008

Ahn K-H, Palmer RN (2016) Use of a nonstationary copula to predict future bivariate low flow frequency in the Connecticut River basin. Hydrol Process 30(19):3518–3532. https://doi.org/10.1002/hyp.10876

Akbari S, Reddy MJ (2020) Non-stationarity analysis of flood flows using copula based change-point detection method: Application to case study of Godavari river basin. Science of the Total Environment 718:134894. https://doi.org/10.1016/j.scitotenv.2019.134894

Bayazit M (2015) Nonstationarity of hydrological records and recent trends in trend analysis: a state-of-the-art review. Environmental Processes 2:527–542. https://doi.org/10.1007/s40710-015-0081-7

Bevacqua E, Maraun D, Vousdoukas MI, Voukouvalas E, Vrac M, Mentaschi L, Widmann M (2019) Higher probability of compound flooding from precipitation and storm surge in Europe under anthropogenic climate change. Science Advances 5:eaaw5531. https://doi.org/10.1126/sciadv.aaw5531

Blanton B, Dresback K, Colle B, Kolar R, Vergara H, Hong Y, Leonardo N, Davidson R, Nozick L, Wachtendorf T (2018) An integrated scenario ensemble-based framework for hurricane evacuation modeling: Part 2-hazard modeling. Risk Anal 40(1):117–133. https://doi.org/10.1111/risa.13004

Brown SJ, Murphy JM, Sexton DMH, Harris GR (2014) Climate projections of future extreme events accounting for modelling uncertainties and historical simulation biases. Clim Dyn 43:2681–2705. https://doi.org/10.1007/s00382-014-2080-1

Cantet P, Arnaud P (2014) Extreme rainfall analysis by a stochastic model: impact of the copula choice on the sub-daily rainfall generation. Stoch Env Res Risk Assess 28(6):1479–1492. https://doi.org/10.1007/s00477-014-0852-0

Chebana F, Ouarda TB (2011) Multivariate quantiles in hydrological frequency analysis. Environmetrics 22(1):63–78. https://doi.org/10.1002/env.1027

Chebana F, Ouarda TB, Duong TC (2013) Testing for multivariate trends in hydrologic frequency analysis. J Hydrol 486:519–530. https://doi.org/10.1016/j.jhydrol.2013.01.007

Cheng L, AghaKouchak A, Gilleland E (2014) Non-stationary extreme value analysis in a changing climate. Clim Change 127:353–369. https://doi.org/10.1007/s10584-014-1254-5

Coles S (2001) An introduction to statistical modeling of extreme values. Springer, London. https://doi.org/10.1007/978-1-4471-3675-0

Dong ND, Agilan V, Jayakumar KV (2019) Bivariate flood frequency analysis of nonstationary flood characteristics. J Hydrol Eng 24(4):04019007. https://doi.org/10.1061/(asce)he.1943-5584.0001770

Du TL, Xiong CY, Xu CJ, Gippel SG, Liu P (2015) Return period and risk analysis of nonstationary low flow series under climate change. J Hydrol 527:234–250. https://doi.org/10.1016/j.jhydrol.2015.04.041

Fang J, Wahl T, Fang J, Sun X, Kong F, Liu M (2020) Compound flood potential from storm surge and heavy precipitation in coastal China. Hydrology and Earth System Sciences Discussions 1–24. 10.5194/hess-2020-377

Faulkner D, Warren S, Spencer P, Sharkey P (2019) Can we still predict the future from the past: Implementing non-stationary flood frequency analysis in the UK. Journal of Flood Risk Management 13(1). https://doi.org/10.1111/jfr3.12582

Feng Y, Shi P, Qu S, Mou S, Chen C, Dong F (2020) Nonstationary flood coincidence risk analysis using time-varying copula functions. Scientific Reports 10(1). https://doi.org/10.1038/s41598-020-60264-3

Ferrer J, P´erez-Mart´ın MA, Jim´enez S, Estrela T, Andreu J, (2012) GIS-based models for water quantity and quality assessment in the j´ucar river basin, Spain, including climate change effects. Sci Total Environ 440:42–59. https://doi.org/10.1016/j.scitotenv.2012.08.032

Fowler HJ, Cooley D, Sain SR, Thurston M (2010) Detecting change in UK extreme precipitation using results from the climate prediction net BBC climate change experiment. Extremes 13:241–267. https://doi.org/10.1007/s10687-010-0101-y

Fréchet M (1928) Sur la lois de probabilité de l'´ecart maximum. Annales de la Societé Polonaise de Mathématique 6:93–122. http://cybra.lodz.pl/Content/6198/AnnSocPolMathe_t.VI_1927.pdf. Accessed 20-01-2022

Galiatsatou P, Makris C, Prinos P, Kokkinos D (2019) Nonstationary joint probability analysis of extreme marine variables to assess design water levels at the shoreline in a changing climate. Nat Hazards 98(3):1051–1089. https://doi.org/10.1007/s11069-019-03645-w

Ganguli P, Merz B (2019) Trends in compound flooding in northwestern Europe during 1901–2014. Geophys Res Lett 46:10810–10820. https://doi.org/10.1029/2019GL084220

Garner AJ, Mann ME, Emanuel KA, Kopp RE, Lin N, Alley RB, Horton BP, DeConto RM, Donnelly JP, Pollard D (2017) Impact of climate change on New York city's coastal flood hazard: Increasing flood heights from the preindustrial to 2300 CE. Proc Natl Acad Sci 114(45):11861–11866. https://doi.org/10.1073/pnas.1703568114

Gilroy KL, McCuen RH (2012) A nonstationary flood frequency analysis method to adjust for future climate change and urbanization. J Hydrol 414–415:40–48. https://doi.org/10.1016/j.jhydrol.2011.10.009

Goharian E, Burian SJ, Bardsley T, Strong C (2016) Incorporating potential severity into vulnerability assessment of water supply systems under climate change conditions. J Water Resour Plan Manag 142(2):04015051. https://doi.org/10.1061/(asce)wr.1943-5452.0000579

Golian S, Saghafian B, Farokhnia A (2012) Copula-based interpretation of continuous rainfall–runoff simulations of a watershed in northern iran. Can J Earth Sci 49(5):681–691. https://doi.org/10.1139/e2012-011

Graler B, van den Berg MJ, Vandenberghe S, Petroselli A, Grimaldi S, Baets BD, Verhoest NEC (2013) Multivariate return periods in hydrology: a critical and practical review focusing on synthetic design hydrograph estimation. Hydrol Earth Syst Sci 17(4):1281–1296. https://doi.org/10.5194/hess-17-1281-2013

Griffin A, Vesuviano G, Stewart E (2019) Have trends changed over time? A study of UK peak flow data and sensitivity to observation period. Nat Hazard 19(10):2157–2167. https://doi.org/10.5194/nhess-19-2157-2019

Gumbel EJ (1958) Statistics of Extremes. Columbia University Press, New York Chichester, West Sussex. https://doi.org/10.7312/gumb92958

Guo E, Zhang J, Si H, Dong Z, Cao T, Lan W (2016) Temporal and spatial characteristics of extreme precipitation events in the Midwest of Jilin province based on multifractal detrended fluctuation analysis method and copula functions. Theoret Appl Climatol 130(1–2):597–607. https://doi.org/10.1007/s00704-016-1909-4

Hafner CM, Manner H (2008) Dynamic stochastic copula models: estimation, inference and applications. METEOR, Maastricht University, Maastricht Research School of Economics of Technology and Organization, METEOR Research Memorandum No.043. https://doi.org/10.26481/umamet.2008043

Hawkes PJ, Gonzalez-Marco D, S´anchez-Arcilla A, Prinos P, (2008) Best practice for the estimation of extremes: A review. J Hydraul Res 46(sup2):324–332. https://doi.org/10.1080/00221686.2008.9521965

Hendry A, Haigh ID, Nicholls RJ, Winter H, Neal R, Wahl T, Joly-Laugel A, Darby SE (2019) Assessing the characteristics and drivers of compound flooding events around the UK coast. Hydrol Earth Syst Sci 23:3117–3139. https://doi.org/10.5194/hess-23-3117-2019

Herdman L, Erikson L, Barnard P (2018) Storm surge propagation and flooding in small tidal rivers during events of mixed coastal and fluvial influence. Journal of Marine Science and Engineering 6(4):158. https://doi.org/10.3390/jmse6040158

Ikeuchi H, Hirabayashi Y, Yamazaki D, Muis S, Ward PJ, Winsemius HC, Verlaan M, Kanae S (2017) Compound simulation of fluvial floods and storm surges in a global coupled river-coast flood model: Model development and its application to 2007 cyclone sidr in bangladesh. Journal of Advances in Modeling Earth Systems 9(4):1847–1862. https://doi.org/10.1002/2017ms000943

Jiang C, Xiong L, Xu CY, Guo S (2014) Bivariate frequency analysis of nonstationary low-flow series based on the time-varying copula. Hydrol Process 29(6):1521–1534. https://doi.org/10.1002/hyp.10288

Kang L, Jiang S, Hu X, Li C (2019) Evaluation of return period and risk in bivariate non-stationary flood frequency analysis. Water 11(1):79. https://doi.org/10.3390/w11010079

Karamouz M, Farzaneh H (2020) Margin of safety based flood reliability evaluation of wastewater treatment plants: Part 2-quantification of reliability attributes. Water Resour Manage 34(6):2043–2059. https://doi.org/10.1007/s11269-020-02543-2

Karamouz M, Fereshtehpour M, Ahmadvand F, Zahmatkesh Z (2016) Coastal flood damage estimator: An alternative to FEMA's HAZUS platform. Journal of Irrigation and Drainage Engineering 142(6). https://doi.org/10.1061/(asce)ir.1943-4774.0001017

Karamouz M, Razmi A, Nazif S, Zahmatkesh Z (2017) Integration of inland and coastal storms for flood hazard assessment using a distributed hydrologic model. Environmental Earth Sciences 76(11). https://doi.org/10.1007/s12665-017-6722-6

Katz RW (2013) Statistical methods for nonstationary extremes. In: A. AghaKouchak, et al., eds. Extremes in a changing climate: detection, analysis and uncertainty. Dordrecht: Springer Science Business media. https://doi.org/10.1007/978-94-007-4479-0

Kirkpatrick JIM, Olbert AI (2020) Modelling the effects of climate change on urban coastal-fluvial flooding. Journal of Water and Climate Change 11(S1):270–288. https://doi.org/10.2166/wcc.2020.166

Kron W (2005) Flood risk = hazard values vulnerability. Water International 30(1):58–68. https://doi.org/10.1080/02508060508691837

Lai Y, Li J, Gu X, Liu C, Chen YD (2021) Global compound floods from precipitation and storm surge: hazards and the roles of cyclones. J Clim 34(20):8319–8339. https://doi.org/10.1175/JCLI-D-21-0050.1

Lee C, Hwang S, Do K, Son S (2019) Increasing flood risk due to river runoff in the estuarine area during a storm landfall. Estuar Coast Shelf Sci 221:104–118. https://doi.org/10.1016/j.ecss.2019.03.021

Li H, Wang D, Singh VP, Wang Y, Wu J, Wu J, Liu J, Zou Y, He R, Zhang J (2019) Nonstationary frequency analysis of annual extreme rainfall volume and intensity using Archimedean copulas: a case study in eastern china. J Hydrol 571:114–131. https://doi.org/10.1016/j.jhydrol.2019.01.054

Libiseller C, Grimvall A (2002) Performance of partial Mann-Kendall tests for trend detection in the presence of covariates. Environmetrics 13(1):71–84. https://doi.org/10.1002/env.507

Lin N, Emanuel K, Oppenheimer M, Vanmarcke E (2012) Physically based assessment of hurricane surge threat under climate change. Nat Clim Chang 2(6):462–467. https://doi.org/10.1038/nclimate1389

Lin N, Kopp RE, Horton BP, Donnelly JP (2016) Hurricane Sandy's food frequency increasing from year 1800 to 2100. PNAS 113(43):12071. https://doi.org/10.1073/pnas.1604386113

Lopez J, Frances F (2013) Non-stationary flood frequency analysis in continental Spanish rivers, using climate and reservoir indices as external covariates. Hydrol Earth Syst Sci 17:3189–3203. https://doi.org/10.5194/hess-17-3189-2013

Lu F, Song X, Xiao W, Zhu K, Xie Z (2020) Detecting the impact of climate and reservoirs on extreme floods using nonstationary frequency models. Stoch Env Res Risk Assess 34:169–182. https://doi.org/10.1007/s00477-019-01747-2

Luo Y, Zhu LS (2019) Investigation of trends in extreme significant wave heights in the South China Sea. Aquat Ecosyst Health Manage 22(1):53–64. https://doi.org/10.1080/14634988.2018.1467194

Machado MJ, Botero BA, L´opez J, Franc´es F, D´ıez-Herrero A, Benito G, (2015) Flood frequency analysis of historical flood data under stationary and non-stationary modelling. Hydrol Earth Syst Sci 12:525–568. https://doi.org/10.5194/hessd-12-525-2015

Manner H, Candelon B (2010) Testing for asset market linkages: A new approach based on time-varying copulas. Pac Econ Rev 15(3):364–384. https://doi.org/10.1111/j.1468-0106.2010.00508.x

Milly PCD, Wetherald RT, Dunne KA, Delworth TL (2002) Increasing risk of great floods in a changing climate. Nature 415(6871):514–517. https://doi.org/10.1038/415514a

Moftakhari HR, Salvadori G, AghaKouchak A, Sanders BF, Matthew RA (2017) Compounding effects of sea level rise and fluvial flooding. Proceedings of the National Academy of Sciences, USA 114:9785–9790. https://doi.org/10.1073/pnas.1620325114

Mudersbach C, Jensen J (2010) Nonstationary extreme value analysis of annual maximum water levels for designing coastal structures on the German north sea coastline. Journal of Flood Risk Management 3(1):52–62. https://doi.org/10.1111/j.1753-318x.2009.01054.x

Nelsen RB (2006) An Introduction to Copulas. Springer, New York. https://doi.org/10.1007/0-387-28678-0

Ouarda TB, Charron C (2019) Changes in the distribution of hydro-climatic extremes in a non-stationary framework. Sci Rep 9:8104. https://doi.org/10.1038/s41598-019-44603-7

Pasquier U, He Y, Hooton S, Goulden M, Hiscock KM (2018) An integrated 1d–2d hydraulic modelling approach to assess the sensitivity of a coastal region to compound flooding hazard under climate change. Nat Hazards 98(3):915–937. https://doi.org/10.1007/s11069-018-3462-1

Patton AJ (2006) Modelling asymmetric exchange rate dependence. Int Econ Rev 47(2):527–556. https://doi.org/10.1111/j.1468-2354.2006.00387.x

Pickands J (1975) Statistical inference using extreme order statistics. The Annals of Statistics 3(1). https://doi.org/10.1214/aos/1176343003

Pirani FJ, Najafi MR (2020) Recent trends in individual and multivariate compound flood drivers in Canada's coasts. Water Resources Research 56(8). https://doi.org/10.1029/2020wr027785

Prosdocimi I, Kjeldsen T (2021) Parametrization of change-permitting extreme value models and its impact on the description of change. Stoch Env Res Risk Assess 35:307–324. https://doi.org/10.1007/s00477-020-01940-8

Razmi A, Golian S, Zahmatkesh Z (2017) Non-stationary frequency analysis of extreme water level: Application of annual maximum series and peak-over threshold approaches. Water Resour Manage 31(7):2065–2083. https://doi.org/10.1007/s11269-017-1619-4

Roussas G (2014) Introduction to Probability 2nd edition. Academic Press, Boston. https://doi.org/10.1016/B978-0-12-800041-0.00014-6

Roux E, Evin G, Eckert N, Blanchet J, Morin S (2020) Non-stationary extreme value analysis of ground snow loads in the French Alps: a comparison with building standards. Nat Hazard 20:2961–2977. https://doi.org/10.5194/nhess2020-81

Saleh F, Ramaswamy V, Wang Y, Georgas N, Blumberg A, Pullen J (2017) A multi-scale ensemble-based framework for forecasting compound coastal-riverine flooding: The hackensack-passaic watershed and Newark bay. Adv Water Resour 110:371–386. https://doi.org/10.1016/j.advwatres.2017.10.026

Sarhadi A, Soulis ED (2017) Time-varying extreme rainfall intensity-duration-frequency curves in a changing climate. Geophys Res Lett 44(5):2454–2463. https://doi.org/10.1002/2016gl072201

Sarhadi A, Burn DH, Aus´ın MC, Wiper MP, (2016) Time-varying nonstationary multivariate risk analysis using a dynamic bayesian copula. Water Resour Res 52(3):2327–2349. https://doi.org/10.1002/2015wr018525

Serinaldi F, Kilsby CG (2015) Stationarity is undead: uncertainty dominates the distribution of extremes. Adv Water Resour 77:17–36. https://doi.org/10.1016/j.advwatres.2014.12.013

Shrestha PL, James SC, Shaller PJ, Doroudian M, Peraza DB, Morgan TA (2014) Estimating the storm surge recurrence interval for hurricane sandy. In World Environmental and Water Resources Congress 2014. American Society of Civil Engineers. https://doi.org/10.1061/9780784413548.191

Singh H, Najafi MR, Cannon AJ (2021) Characterizing non-stationary compound extreme events in a changing climate based on large-ensemble climate simulations. Clim Dyn 56:1389–1405. https://doi.org/10.1007/s00382-020-05538-2

Singh VP, Strupczewski WG (2002) On the status of flood frequency analysis. Hydrol Process 16(18):3737–3740. https://doi.org/10.1002/hyp.5083

Sklar A (1959) Fonctions de répartition à n dimensions et leurs marges. Publications de l´Institut de Statistique de l' Université de Paris 8:229–231

Song JB, Wei EB, Hou YJ (2004) Joint statistical distribution of two-point sea surface elevations in finite water depth. Coast Eng 50(4):169–179. https://doi.org/10.1016/j.coastaleng.2003.09.006

Svensson C, Kundzewicz WZ, Maurer T (2005) Trend detection in river flow series: 2. flood and low-flow index series / d´etection de tendance dans des s´eries de d´ebit fluvial: 2. s´eries d'indices de crue etd'´etiage. Hydrological Sciences Journal 50(5). https://doi.org/10.1623/hysj.2005.50.5.811

Tsakiris G, Kordalis N, Tsakiris V (2015) Flood double frequency analysis: 2d-archimedean copulas vs bivariate probability distributions. Environmental Processes 2:705–716. https://doi.org/10.1007/s40710-015-0078-2

Wahl T, Jain S, Bender J, Meyers SD, Luther ME (2015) Increasing risk of compound flooding from storm surge and rainfall for major US cities. Nat Clim Chang 5(12):1093–1097. https://doi.org/10.1038/nclimate2736

Wahlin K, Grimvall A (2009) Roadmap for assessing regional trends in groundwater quality. Environ Monit Assess 165(1–4):217–231. https://doi.org/10.1007/s10661-009-0940-7

Wang S (2020) Uncertainties in the assessment of individual and compound flooding from river discharge and coastal water levels under climate change. Electronic Thesis and Dissertation Repository: 551, University of Western Ontario. https://ir.lib.uwo.ca/etd/7551. Accessed 20-01-2022

Wen T, Jiang C, Xu X (2019) Nonstationary analysis for bivariate distribution of flood variables in the Ganjiang river using time-varying copula. Water 11(4):746. https://doi.org/10.3390/w11040746

Xavier ACF, Blain GC, Morais MV, Sobierajski GR (2019) Selecting "the best" nonstationary Generalized Extreme Value (GEV) distribution: on the influence of different numbers of GEV-models. Bragantia 78(4):606–621. https://doi.org/10.1590/1678-4499.20180408

Xu K, Ma C, Lian J, Bin L (2014) Joint probability analysis of extreme precipitation and storm tide in a coastal city under changing environment. PLoS ONE 9(10):e109341. https://doi.org/10.1371/journal.pone.0109341

Xu P, Wang D, Singh VP, Wang Y, Wu J, Lu H, Wang L, Liu J, Zhang J (2019) Time-varying copula and design life level-based nonstationary risk analysis of extreme rainfall events. Hydrology and Earth System Sciences, Accepted Manuscript. https://doi.org/10.5194/hess-2019-358

Yan L, Xiong L, Guo S, Xu C-Y, Xia J, Du T (2017) Comparison of four nonstationary hydrologic design methods for changing environment. J Hydrol 551:132–150. https://doi.org/10.1016/j.jhydrol.2017.06.001

Ye F, Zhang Y, Yu H, Sun W, Moghimi S, Myers E, Nunez MK, Zhang R, Wang H, Roland A, Martins K, Bertin X, Du J, Liu Z (2019) Simulating storm surge and compound flooding events with a

creek-to-ocean model: Importance of baroclinic effects. Ocean Model 145:101526. https://doi.org/10.1016/j.ocemod.2019.101526
Yoon J-H, Wang S-YS, Gillies RR, Kravitz B, Hipps L, Rasch PJ (2015) Increasing water cycle extremes in California and in relation to ENSO cycle under global warming. Nature Communications 6(1). https://doi.org/10.1038/ncomms9657
Zahmatkesh Z, Burian SJ, Karamouz M, Tavakol-Davani H, Goharian E (2015a) Low-impact development practices to mitigate climate change effects on urban stormwater runoff: Case study of New York City. J Irrig Drain Eng 141(1):04014043. https://doi.org/10.1061/(asce)ir.1943-4774.0000770
Zahmatkesh Z, Karamouz M, Goharian E, Burian SJ (2015b) Analysis of the effects of climate change on urban storm water runoff using statistically downscaled precipitation data and a change factor approach. J Hydrol Eng 20(7):05014022. https://doi.org/10.1061/(asce)he.1943-5584.0001064
Zellou B, Rahali H (2019) Assessment of the joint impact of extreme rainfall and storm surge on the risk of flooding in a coastal area. J Hydrol 569:647–665. https://doi.org/10.1016/j.jhydrol.2018.12.028
Zhang T, Wang Y, Wang B, Tan S, Feng P (2018) Nonstationary flood frequency analysis using univariate and bivariate time-varying models based on GAMLSS. Water 10(7):819. https://doi.org/10.3390/w10070819
Zhang YJ, Ye F, Yu H (2020) Simulating compound flooding events in a hurricane. Ocean Dyn 70:621–640. https://doi.org/10.1007/s10236-020-01351-x
Zscheischler J, Westra S, van den Hurk BJJM, Seneviratne SI, Ward PJ, Pitman A, AghaKouchak A, Bresch DN, Leonard M, Wahl T, Zhang X (2018) Future climate risk from compound events. Nat Clim Chang 8(6):469–477. https://doi.org/10.1038/s41558-018-0156-3

Authors and Affiliations

Ali Razmi[1] · Heydar Ali Mardani-Fard[2] · Saeed Golian[1,3] · Zahra Zahmatkesh[4]

Ali Razmi
ali.razmi@shahroodut.ac.ir

Saeed Golian
s.golian@shahroodut.ac.ir

Zahra Zahmatkesh
zhr_zahmatkesh@yahoo.com

[1] Civil Engineering Department, Shahrood University of Technology, Shahrood, Iran

[2] Department of Mathematics, Yasouj University, Yasouj, Iran

[3] Department of Geography, Maynooth University, Maynooth, Ireland

[4] Department of Civil Engineering, McMaster University, Hamilton, ON L8S4L8, Canada